

Self-consistent rate-equation approach to transitions in critical island size in metal (100) and metal (111) homoepitaxy

Mihail N. Popescu, Jacques G. Amar,* and Fereydoon Family
Department of Physics, Emory University, Atlanta, Georgia 30322

(Received 25 September 1997)

A self-consistent rate-equation approach to the study of transitions in the critical island size i in submonolayer growth from $i=1$ to $i=2$ and from $i=1$ to $i=3$, corresponding to homoepitaxial growth on metal (111) and (100) surfaces, is presented. In contrast to previous standard rate-equation results, the average island density and monomer density are well predicted along with the transition temperature from $i=1$ to a higher critical island size. It is shown that the method's implicit short-range correlations between attachment/detachment rates, together with a careful estimate of the escape rates for small clusters, are important factors for a good agreement with the kinetic Monte Carlo simulation results. [S0163-1829(98)00227-6]

I. INTRODUCTION

The development of new experimental techniques, such as scanning tunneling microscopy (STM), and reflection high-energy electron diffraction (RHEED), has made possible the real-time probing of microscopic details of the surface during the early stages of thin-film growth.¹ These developments have renewed both the experimental²⁻¹² and theoretical¹³⁻²² interest in the scaling properties of the island density and island-size distribution in submonolayer epitaxial growth. One motivation is that the dependence of the submonolayer island density N on deposition rate and temperature at fixed coverage θ in the precoalescence regime may be used to identify important activation energies for microscopic processes on the surface.

One concept that has been extensively used in such studies is that of a critical island size i (Ref. 13) corresponding to one less than the number of atoms in the smallest stable island. According to the standard rate-equation (RE) analysis¹³ for a given critical island size i , the island density N (at fixed coverage θ) scales as

$$N \sim (D_h/F)^{-\chi_i} e^{E_i/(i+2)k_B T}, \quad (1)$$

where F is the deposition rate, $D_h = \nu_0 e^{-E_a/k_B T}$ is the hopping rate (where ν_0 is the attempt frequency and E_a is the activation energy for adatom diffusion), E_i is the critical cluster binding energy, and $\chi_i = i/(i+2)$. With increasing temperature, a transition from a critical island size $i=1$ at low temperature to a higher critical island size at high temperature is expected to occur. In particular, such transitions have been observed in metal (111) and metal (100) homoepitaxy for a variety of systems.^{6,8,9,12} For example, a transition from $i=1$ at room temperature to $i=3$ at higher temperature was reported for Fe/Fe(100) deposition.⁸ Recently, a transition from $i=1$ to $i=2$ with increasing temperature has also been reported in Rh/Rh(111) deposition.¹²

One of the standard tools used in studying submonolayer growth is the rate-equation approach.²³ Rate equations with constant or power-law size-dependent capture numbers have been successfully used to predict the qualitative behavior of

the dependence of island and monomer density on the deposition flux and on coverage.¹³⁻¹⁵ However, it has been shown^{14,15} that this standard approach cannot give *quantitative* agreement with the experimental data or kinetic Monte Carlo (KMC) simulations.

Recently, Bales and Chrzan carried out a self-consistent calculation of the rate coefficients for the case of irreversible low-temperature growth²⁰ (corresponding to $i=1$) that gives quantitative agreement with KMC simulations. In addition, Bales and Zangwill²¹ have recently suggested a generalization of the self-consistent rate-equation calculation for the case of reversible growth corresponding to growth at higher temperature. Using this approach, good agreement was found with Monte Carlo simulations for a model with no critical island size and a detachment rate that decreased very slowly with the island size.

In the present work we consider a RE approach to submonolayer growth for a restricted pair-bond model^{16,22} that is relevant to low- and intermediate-temperature metal (100) and (111) homoepitaxy. Our model is very different from the one studied in Ref. 21 since in our model only small islands are unstable, while in the model studied in Ref. 21 all islands are unstable and there is no critical island size. We note that in previous work²² we have shown that for this model the standard RE approach¹⁷ leads to poor agreement with KMC simulations, as well as to a prediction for the crossover scaling function, which significantly *underestimates* the transition temperature. It was suggested²² that this is due to the lack of a self-consistent treatment of attachment/detachment in that approach. Here we focus on a rate-equation approach in which a self-consistent calculation of the attachment and escape rates is used. We also compare our results with new KMC simulations. As discussed in more detail below, our results indicate that such an approach leads to good agreement with KMC simulation results for the average monomer density, island density, and crossover scaling behavior.

The organization of this paper is as follows. After a brief discussion of the model and of the crossover scaling form for the island density for the case of reversible growth, we present the details of our self-consistent rate-equation ap-

proach. We then present a comparison between our rate-equation predictions and KMC simulations. A summary of our results and conclusions are presented in Sec. V.

II. RESTRICTED PAIR-BOND MODEL AND SCALING OF THE ISLAND DENSITY

The restricted pair-bond model considered here has been previously studied via KMC simulations^{16,19,22} and standard RE analysis¹⁷⁻²² and is described by the following rules: (a) Adatoms without a nearest-neighbor bond (monomers) may randomly diffuse (hop) to a nearest-neighbor site with hopping rate D_h . (b) Adatoms with one nearest-neighbor bond may diffuse to a nearest-neighbor site with detachment rate $D_1 = r_1 D_h$, where $r_1 = e^{-E_N/k_B T}$ and E_N is the nearest-neighbor bond energy. (c) Enhanced edge diffusion is included such that adatoms with just one nearest neighbor bond may diffuse along edges and around kinks with a rate $D_e = r_e D_h$. (d) Atoms with two or more nearest-neighbor bonds are assumed to be immobile.

As already noted, this model is appropriate for homoepitaxial growth on (100) and (111) metal surfaces at temperatures for which two-bond detachment may be neglected.¹⁴ At low temperatures (corresponding to stable dimers) the critical island size i is equal to 1. However, with increasing temperature dimers become unstable, leading to an increased critical island size. In particular, at high temperatures on a triangular lattice [corresponding to a (111) metal surface] trimers will be stable, corresponding to $i=2$. Similarly, at high temperatures on a square lattice [corresponding to a (100) metal surface] tetramers will be stable, corresponding to $i=3$.

Of particular interest is the crossover behavior as a function of temperature from $i=1$ to a higher critical island size $i=2(3)$ on triangular (square) lattices. A general crossover scaling form for a transition from a critical island size $i=1$ to $i=k$ in the absence of two-bond detachment has already been proposed,¹⁶

$$N \sim R^{-1/3} f_{1k}(r_1^{x_{1k}} R), \quad (2)$$

where N is the island density at fixed coverage θ , $R = D_h/F$, and the crossover scaling function f_{1k} satisfies

$$f_{1k}(u) \sim \begin{cases} \text{const} & \text{for } u \ll 1 \\ u^{-2(k-1)/[3(k+2)]} & \text{for } u \gg 1. \end{cases} \quad (3)$$

For our model, the standard RE result (1) along with a consideration of the binding energy of the critical island implies $x_{1k} = 3/2$ for $k=2,3$.^{17,22} We note that recent KMC simulations²² on a triangular lattice have shown good agreement with this result ($x_{12} \approx 3/2$), while on a square lattice a slightly lower effective value has been found ($x_{13} \approx 1.33$).

The crossover scaling form (2) also implies that the effective scaling exponent $\chi = d(\ln N)/d(\ln F)$ may be written in a similar form,

$$\chi(r_1, R) = g_{1k}(r_1^{x_{1k}} R), \quad (4)$$

where the crossover scaling function g_{1k} satisfies

$$g_{1k}(u) = \begin{cases} 1/3 & \text{for } u \ll 1 \\ \frac{k}{k+2} & \text{for } u \gg 1. \end{cases} \quad (5)$$

As already noted,²² the standard RE approach¹⁷ leads to poor agreement for both the island-density crossover scaling function f_{1k} and the effective exponent crossover scaling function g_{1k} and significantly underestimates the transition temperature. Accordingly, in the present work we focus on a self-consistent approach. However, before discussing this approach in detail, we first briefly describe our kinetic Monte Carlo (KMC) simulations of the restricted pair-bond model.

As in previous work^{15,16,19,22} simulations were carried out using a simple solid-on-solid (SOS) model with square and triangular lattices. In both cases, adatoms were deposited starting with an initially flat surface at a rate F per site while deposited adatoms without a nearest-neighbor in-plane bond (monomers) were allowed to diffuse randomly to nearest-neighbor sites with hopping rate D_h . Adatoms with one or more nearest-neighbor in-plane bonds were allowed to diffuse as described above. In particular, for the case of rapid edge-diffusion on a triangular lattice, adatoms with one nearest-neighbor bond were allowed to diffuse ‘‘along an edge’’ (i.e., to a nearest-neighbor site that retained a bond with the original bond site) at a rate $D_e = D_h$. For the case of rapid edge diffusion on a square lattice, adatoms with one nearest-neighbor bond were allowed to diffuse ‘‘along an edge’’ and around ‘‘corners’’ at a rate $D_e = D_h$ in order to mimic rapid cluster relaxation. For both triangular and square lattices the edge diffusion of dimer atoms was suppressed in order to prevent dimer mobility.

In addition to adatoms that land directly on the surface, adatoms may land on an existing island. In this case the deposited adatoms are assumed to diffuse in the same manner as on the substrate, while monomers may diffuse over an island edge to the layer below at the same rate as for ordinary diffusion.²⁴ Thus, for example, an adatom that lands on another adatom will almost immediately ‘‘diffuse’’ to the layer below and form a dimer.

In order to obtain good statistics for both the island density N (corresponding to the density of clusters of size 2 or larger) and the monomer density $\langle n_1 \rangle$, averages were carried out over 10–30 runs, using lattice sizes ranging from $L = 500$ to $L = 1000$. In order to study transitions in the critical island size as a function of temperature, the average island and monomer densities were measured in the submonolayer ‘‘precoalescence’’ regime ($0 \leq \theta \leq 0.3$) using a wide range of values for the one-bond detachment rate r_1 ($2.5 \times 10^{-6} < r_1 < 10^{-3}$) and diffusion ratio $R = D_h/F$ ($10^5 < R < 10^{11}$).

III. SELF-CONSISTENT RATE-EQUATION APPROACH

The rate-equation approach^{13,23} involves a set of deterministic coupled reaction-diffusion equations describing the time (coverage) dependence of average quantities. The RE variables are the average densities of monomers $\langle n_1 \rangle$ and of islands of size $s \geq 2$, $\langle n_s \rangle$, where s is the number of atoms in the island. A general form of these equations, taking into account nucleation and aggregation of islands, direct impingement of adatoms, and detachment of monomers from unstable islands may be written as

$$\begin{aligned} \frac{d\langle n_1 \rangle}{d\theta} &= 1 - 2k_1\langle n_1 \rangle - \sum_{s \geq 2} k_s \langle n_s \rangle - 2\frac{R}{4}\sigma_1\langle n_1 \rangle^2 \\ &\quad - \frac{R}{4}\langle n_1 \rangle \sum_{s \geq 2} \sigma_s \langle n_s \rangle + 2F^{-1}\frac{\langle n_2 \rangle}{\tau_2} + F^{-1} \sum_{s \geq 3} \frac{\langle n_s \rangle}{\tau_s}, \end{aligned} \quad (6a)$$

$$\begin{aligned} \frac{d\langle n_s \rangle}{d\theta} &= \frac{R}{4} \langle n_1 \rangle (\sigma_{s-1}\langle n_{s-1} \rangle - \sigma_s \langle n_s \rangle) + k_{s-1}\langle n_{s-1} \rangle \\ &\quad - k_s \langle n_s \rangle - F^{-1}\frac{\langle n_s \rangle}{\tau_s} + F^{-1}\frac{\langle n_{s+1} \rangle}{\tau_{s+1}}, \quad \text{for } s \geq 2. \end{aligned} \quad (6b)$$

In these equations, the terms with σ_s correspond to the capture of monomers by other monomers or by existing islands, while the terms with τ_s^{-1} correspond to the detachment of monomers from islands of size s . The terms with k_s (where $k_s = s$ since diffusion is much faster than deposition) correspond to the deposition of adatoms directly on islands of size s . The factors of 1/4 in the capture terms are included since these terms are usually expressed in terms of the diffusion constant D rather than of the hopping rate D_h ($D = D_h/4$ for both square and triangular lattices).

Of crucial importance in the use of rate equations as a tool to make quantitative predictions is an accurate calculation of the capture numbers σ_s and escape rates τ_s^{-1} . As has already been mentioned, the restricted pair-bond model gives a realistic description of a critical island size transition on metal (100) and (111) surfaces. In this model only the small islands (dimers and trimers) are unstable; therefore a careful calculation of the attachment/detachment rates for these small islands is required.

Recently, Bales and Zangwill²¹ have outlined a mean-field procedure for the self-consistent calculation of the capture numbers and detachment rates. Essentially, this consists of solving a diffusion equation for the monomer density $n_1(r)$ near an island of size s of the form,

$$\nabla^2 n_1(\mathbf{r}) - \xi^{-2}[n_1(\mathbf{r}) - \langle n_1 \rangle] = 0, \quad (7)$$

where the screening (absorption) length ξ corresponding to the effect of all the other islands and monomers is given by

$$\xi^{-2} = (4/R)k_1 + 2\sigma_1\langle n_1 \rangle + \sum_{s \geq 2} \sigma_s \langle n_s \rangle. \quad (8)$$

Assuming radial symmetry and the boundary condition that far from the island the monomer density takes the average value $\langle n_1 \rangle$, the solution of Eq. (7) is

$$n_1(r) = \langle n_1 \rangle - AK_0(r/\xi), \quad (9)$$

where K_0 is the zeroth-order modified Bessel function, and the constant A is determined by the boundary condition at the edge of the island.

Of crucial importance is a correct boundary condition for the monomer density $n_1(r)$ at the island edge $r = R_s$ (where R_s is the radius of a circular island of size s and is typically

assumed to satisfy²⁰ $R_s = \alpha s^{1/d_f}$ with d_f the fractal dimension of the island and α close to 1). Bales and Zangwill²¹ have considered the following form connecting the macroscopic flux at the island boundary with the microscopic attachment/detachment rates:

$$2\pi R_s(D_h/4)\frac{\partial n_1(R_s)}{\partial r} = m_s(D_h/4)n_1(R_s + a) - J_s, \quad (10)$$

where $J_s = \omega_{s+1}\langle n_{s+1} \rangle / \langle n_s \rangle$ is the detachment rate at the edge of an island of size s , $a = 1$ is the lattice constant, m_s is the number of paths connecting next-nearest-neighbor sites to nearest-neighbor sites on the perimeter, and ω_{s+1} is the effective detachment rate from an island of size $s+1$. The factor of 1/4 in the capture term is appropriate only for a square lattice geometry and in general should be replaced by one over the total number of hopping directions. A Taylor expansion of the monomer density near R_s leads to the boundary condition,

$$\frac{\partial n_1(R_s)}{\partial r} = \beta_s[n_1(R_s) - n_{eq}(R_s)], \quad (11)$$

with $n_{eq}(R_s) = J_s / (m_s D_h/4)$ and $\beta_s^{-1} = (2\pi R_s / m_s) - 1$.

Equations (9) and (11) may be used to compute the microscopic form of the flux $2\pi R_s(D_h/4)[\partial n_1(R_s)/\partial r]$ at the island edge. Equating this to the RE form,

$$(D_h/4)\sigma_s \langle n_1 \rangle - \frac{\langle n_{s+1} \rangle}{\tau_{s+1}\langle n_s \rangle}, \quad (12)$$

the following expressions for the capture numbers and escape rates are obtained:²¹

$$\sigma_s = \frac{2\pi R_s K_1(R_s/\xi)}{\beta_s^{-1} K_1(R_s/\xi) + \xi K_0(R_s/\xi)}, \quad (13a)$$

$$\tau_2^{-1} = \frac{\omega_2 \sigma_1}{2m_1}; \quad \tau_{s+1}^{-1} = \frac{\omega_{s+1} \sigma_s}{m_s}, \quad s \geq 2, \quad (13b)$$

where K_0, K_1 are modified Bessel functions.²⁵ The extra factor of 2 (which was not explicitly noted in Ref. 21) in the expression for τ_2^{-1} is due to the fact that two monomers are produced by the breakup of a dimer.²⁶

We note that in the above discussion we have used the same form for the microscopic detachment rate J_s as in Ref. 21. The alternative form $J_s = \omega_s$ (in which the outward flux corresponds directly to the detachment rate from an island of size s) may also be used and was found to give similar results. This leads to the same expression for σ_s , but a modified one for the escape rates,

$$\tau_2^{-1} = \frac{\omega_2 \sigma_2}{2m_2}; \quad \tau_s^{-1} = \frac{\omega_s \sigma_s}{m_s}, \quad s \geq 3. \quad (13c)$$

For the case of low-temperature irreversible growth ($\omega_s = 0$) the correct boundary condition in the absence of a barrier to attachment is $n_1(R_s) = 0$, which leads to the constraint $\beta_s^{-1} = 0$. In the previous work of Bales and Zangwill,²¹ this

was accomplished by assuming that $m_s \approx 2\pi R_s$ for all s and studying a model in which the islands were forced to be circular. In contrast, in our model this is a poor approximation—and leads to poor agreement with KMC simulations—since detachment is only allowed from small islands. On the other hand, a direct counting of m_s for small islands leads to $\beta_s^{-1} < 0$, which is unphysical.

In order to solve these problems, we have carried out the following procedure. First, the attachment term corresponding to the first term on the right-hand side of Eq. (10) has been replaced with a sum over all sites one hop away from the perimeter sites. Carrying out a Taylor expansion, this leads to the following expression for β_s^{-1} ,

$$\beta_s^{-1} = \left[2\pi R_s(M/4) - \sum_{\langle j \rangle} \bar{x}_j m_s^j \right] / m_s, \quad (14)$$

where the sum runs over all sites j that are within one hop of an attachment site, m_s^j is the number of paths connecting such a site with a perimeter site, and $m_s = \sum_j m_s^j$. In the above expression, M is the number of hopping directions ($M=4$ on a square lattice, $M=6$ on a triangular lattice) and \bar{x}_j is the difference between the distance x_j from the site j to the center of the island and R_s . The constraint $\beta_s^{-1} = 0$ then leads to the following expression for the “effective” radius R_s ,

$$R_s = \frac{\sum_j x_j m_s^j}{m_s + \pi M/2}. \quad (15)$$

For example, on a square lattice, for a monomer there are four next-nearest-neighbor sites at a distance $2a$, and four next-nearest-neighbor sites at a distance $a\sqrt{2}$. Equation (15) then leads to $R_1 = 4a(1 + \sqrt{2})/(6 + \pi)$. A similar calculation has been done for the small unstable islands on both triangular and square lattices. We note that the radius values obtained from Eq. (15) are not significantly different from the previously mentioned values $R_s = s^{1/d_f}$. However, the use of the correct value of m_s in Eq. (13b) is of crucial importance for the correct estimate of the escape rates for the restricted pair-bond model and is theoretically consistent with Eq. (11) only if the radius is redefined as in Eq. (15). For larger islands, for which both corrections in R_s and detachment are negligible in our model, the usual expression²⁰ $R_s = s^{1/d_f}$ was used along with the continuum approximation $m_s = 2\pi R_s$.

IV. RESULTS

A. Triangular lattice geometry

Figure 1 shows typical results for the average monomer density and total island density (corresponding to the density of clusters of size 2 or larger) as a function of coverage obtained using our self-consistent RE approach for the restricted pair-bond model on a triangular lattice corresponding to growth on a metal (100) surface. The results span a range of values of the crossover variable $Y = r_1^{3/2}R$ as well as of the critical island size ranging from $i=1$ to $i=2$. Also shown are KMC simulation results with the same parameters for the

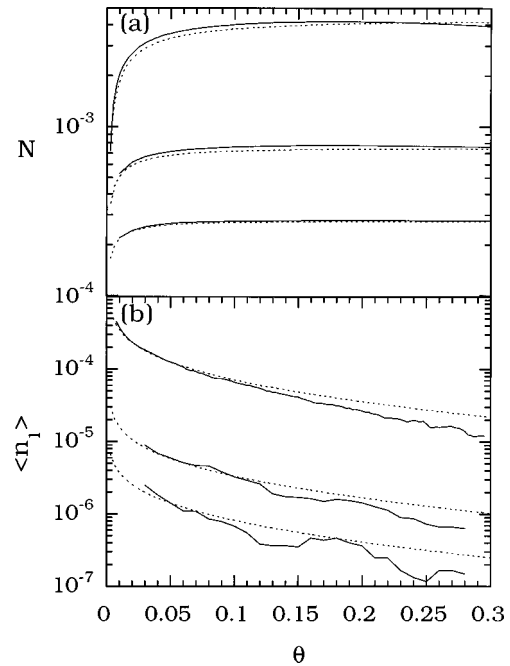


FIG. 1. KMC (solid lines) and RE (dotted lines) results for the island density (a) and for the monomer density (b) as a function of coverage on a triangular lattice for different values of the scaling variable Y . From top to bottom, $r_1 = 2.15 \times 10^{-5}$, $R = 10^6$ ($Y \approx 0.1$); $r_1 = 2.15 \times 10^{-5}$, $R = 10^8$ ($Y \approx 10$); $r_1 = 2.15 \times 10^{-5}$, $R = 10^9$ ($Y \approx 100$).

case of large edge diffusion. As can be seen, in contrast to the standard rate-equation results,^{17,22} there is very good agreement between the self-consistent rate-equation results and the KMC simulations for both the island and the monomer densities. We note that in the rate equations we assumed that islands with size $s \geq 3$ are stable, which corresponds to the case of large edge diffusion (see Appendix). The fractal dimension used in the RE was $d_f = 1.8$, since it has been previously shown^{19,27} that on a triangular lattice the islands remain fractal in the absence of two-bond detachment.

We have also calculated the effective exponent $\chi = d(\ln N)/d(\ln F)$ using our self-consistent rate-equation approach as a function of the crossover scaling variable Y as shown in Fig. 2. Also shown are previously published KMC results²² both with and without edge diffusion. For comparison, we have also included the standard RE results, as well as RE results using capture cross sections appropriate for the irreversible case,²⁰ but without a self-consistent calculation of the escape rates. As can be seen, while there is very good agreement between the self-consistent RE results and KMC simulations, the other RE approaches significantly underestimate the crossover temperature. The improved agreement of the self-consistent RE approach shows clearly that the correlation between attachment and detachment rates, as expressed in Eq. (13b), is the key factor in obtaining correct results. We note that the values of r_1 , R , and Y , used in the RE results shown in Fig. 2 correspond to typical values for metal (111) deposition.¹²

While our self-consistent rate-equation results for χ agree well with the KMC simulation results, in the limit of large Y ($Y \approx 10^5$) they appear to slightly overshoot the classical value $\chi = 1/2$ corresponding to $i=2$. Similar behavior can be observed in the RE results corresponding to a variable capture cross section without self-consistent detachment (dashed

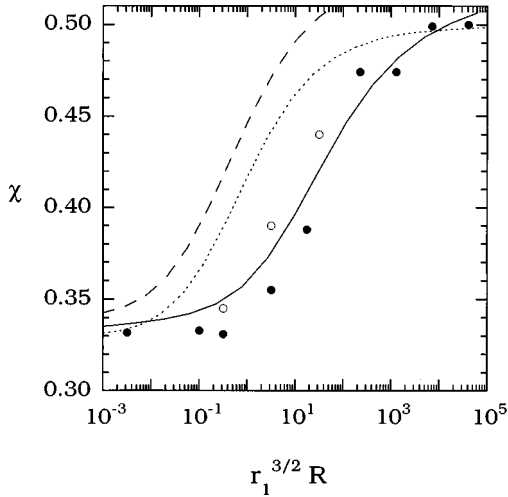


FIG. 2. Island-density scaling exponent $\chi = d(\ln N)/d(\ln F)$ as a function of the scaling variable $Y = r_1^{3/2}R$ on a triangular lattice. Filled symbols correspond to KMC results with $D_e = 0$ (no edge-diffusion), open symbols correspond to KMC results with $D_e = D_h$ (rapid edge diffusion). The solid line corresponds to the self-consistent RE prediction, the dashed line to the standard RE with variable capture numbers, and the dotted line to the standard RE with constant capture numbers.

line) although not for the standard RE results (dotted line). The most likely explanation for this is the existence of logarithmic corrections which arise in the self-consistent rate-equation approach²⁰ but which are effectively screened due to correlations. For large $R = D_h/F$ these corrections are very small (as can be seen from Fig. 2) and vanish in the limit of infinite R . However, given the smallness of the overshoot it is also possible that slight numerical inaccuracies that arise in the integration of the self-consistent rate equations for large R may play a role.

B. Square lattice geometry

Figures 3 and 4 show similar results to those in Fig. 1 for the case of reversible growth on a square lattice [corresponding to growth on a metal (100) surface] both for the case without edge diffusion (Fig. 3) as well as with rapid edge diffusion (Fig. 4). The results span a range of values of the crossover variable $Y = r_1^{x_{13}}R$ ranging from small Y (corresponding to $i=1$) to large Y (corresponding to $i=3$). In this case, the fractal dimension used was $d_f = 2.0$ since even without edge diffusion the islands are compact due to detachment. As can be seen in Fig. 3, for the case of no edge diffusion there is excellent agreement between the self-consistent RE predictions and the KMC results. We note that the fluctuations observed in the KMC results are due to the very low monomer density that leads to poor statistics. Also shown (Fig. 4) are the results obtained for the case of rapid edge diffusion. In this case the island density is somewhat overestimated by the RE, although the monomer density is still well predicted.²⁸

We note that for the RE results shown here we have assumed that islands with four or more atoms are stable. This is a good approximation for the case with rapid edge diffusion since in this case any atom that attaches to an island can

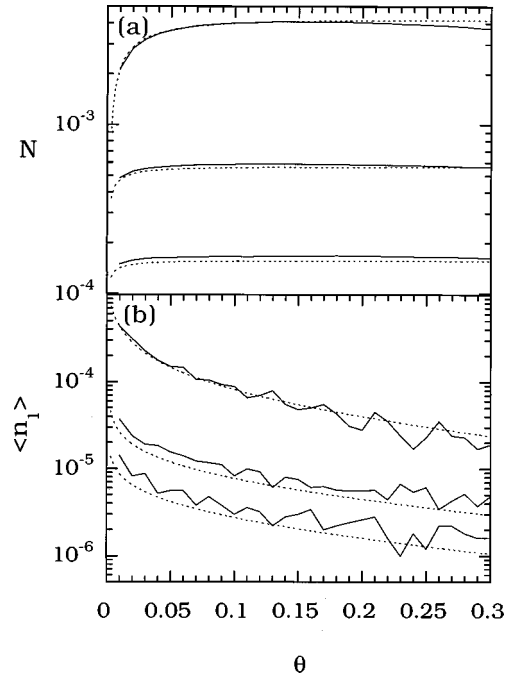


FIG. 3. KMC (solid lines) and RE (dotted lines) results for the island density (a) and for the monomer density (b) as a function of coverage for different values of the scaling variable Y on a square lattice for the case of no edge diffusion ($D_e = 0$). From top to bottom, $r_1 = 10^{-4}$, $R = 10^6$ ($Y \approx 4.6$); $r_1 = 10^{-4}$, $R = 10^8$ ($Y \approx 460$); $r_1 = 10^{-4}$, $R = 10^9$ ($Y \approx 4600$).

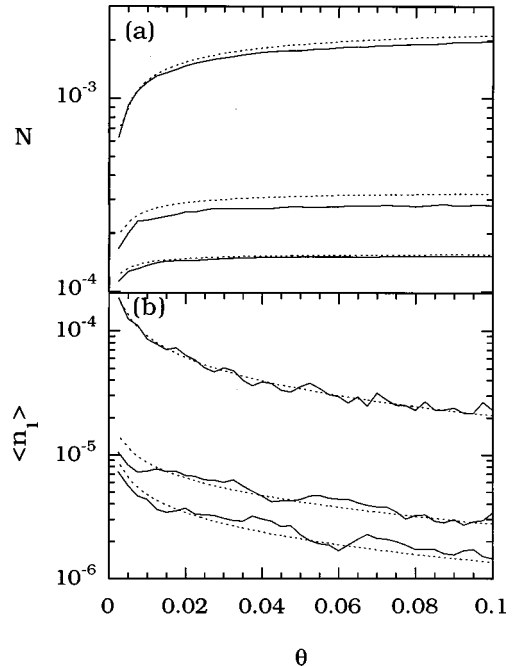


FIG. 4. KMC (solid lines) and RE (dotted lines) results for the island density (a) and for the monomer density (b) as a function of coverage for different values of the scaling variable Y on a square lattice for the case of rapid edge diffusion ($D_e = D_h$). From top to bottom, $r_1 = 10^{-5}$, $R = 10^7$ ($Y \approx 2$); $r_1 = 10^{-5}$, $R = 10^9$ ($Y \approx 200$); $r_1 = 10^{-4}$, $R = 10^9$ ($Y \approx 4600$).

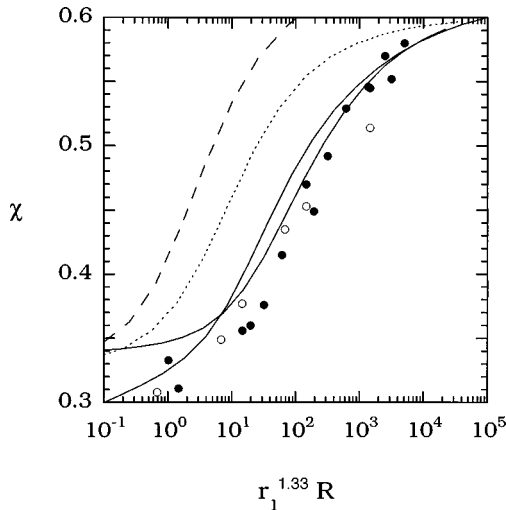


FIG. 5. Island-density scaling exponent $\chi = d(\ln N)/d(\ln F)$ as a function of the scaling variable $Y = r_1^{1.33}R$ on a square lattice. Filled symbols correspond to KMC results with $D_e = 0$ (no edge diffusion), open symbols correspond to KMC results with $D_e = D_h$ (rapid edge diffusion). The solid lines correspond to the self-consistent RE predictions with higher D_h/F for small Y (upper curve) and lower D_h/F for small Y (lower curve). The dashed line corresponds to the standard RE results with variable capture numbers, while the dotted line corresponds to RE results with constant capture numbers.

immediately find a stable binding site. Therefore, it is rather surprising that we find good agreement for both the case *without* edge diffusion and *with* edge diffusion. As previously noted in Ref. 29 this appears to be due to the fact that while monomers that attach to an island may detach in the case without edge diffusion, they are very likely to quickly reattach to the same island at a stable binding site and so do not lead to a significant modification of the rate equations. We note that in our calculations we also considered the case in which detachment from islands of sizes 5 and 7 was allowed (see Appendix) since for these island sizes at least one atom may detach. However, this led to results that were not significantly different from those already shown.

We have also used our self-consistent rate-equation approach to calculate the exponent χ as a function of the crossover scaling variable Y as shown in Fig. 5.³⁰ The parameters used were again chosen to be typical for metal (100) deposition.¹⁷ In particular, we have included two RE curves, one corresponding to small D_h/F at low temperatures ($\nu_0/F = 5 \times 10^{11}$, $E_a = 0.4$ eV, $E_N = 0.2$ eV, $200 \text{ K} < T < 350 \text{ K}$) the other corresponding to a higher value of D_h/F for the same value of Y ($\nu_0/F = 10^{13}$, $E_a = 0.45$ eV, $E_N = 0.6$ eV, $380 \text{ K} < T < 700 \text{ K}$). As can be seen, for large Y (corresponding to high temperatures) there is very little difference between the two RE curves. However, for the small D_h/F case the effective value of χ is lower for small Y (low temperature) than the expected value of $1/3$ due to the fact that the corresponding D_h/F values are not in the asymptotic scaling range. Also shown are previously published KMC results for χ (Ref. 22) both with and without edge diffusion. As for the triangular lattice, there is now very good agreement between the self-consistent rate-equation results and KMC simulations, although again there appears to be the possibility of a very slight overshoot in the value of χ for very large Y .

For comparison, Fig. 5 also shows the standard RE results with constant capture cross section, as well as RE results using capture cross section appropriate for the irreversible case but without a self-consistent calculation of the escape rates. In contrast to our self-consistent RE results, these results show a very poor agreement with the simulations. Therefore, we conclude again that the improved agreement is due to the use of a self-consistent calculation of the attachment/detachment rates for small islands.

V. CONCLUSIONS

We have used a self-consistent rate-equation approach to study a model of submonolayer growth that is relevant to low- and intermediate-temperature metal (100) and (111) homoepitaxy. We have also studied the crossover behavior in the island density as a function of temperature for this model. Good agreement was found with KMC simulations for both the monomer and island densities as well as for the island-density scaling exponent χ for both triangular and square lattices. This is in contrast to previous approaches¹⁷ that gave poor agreement for both the island and monomer densities and greatly underestimated the transition temperature.

Of key importance in obtaining good agreement with the KMC simulations was the use of a self-consistent calculation of attachment and escape rates. Such a calculation implicitly takes into account short-range correlations between attachment and detachment processes. This leads to a ‘‘correction’’ factor σ_s/m_s that multiplies the microscopic detachment rate and gives the reduced effective escape rate τ_s^{-1} .²¹ We note that such a factor is equivalent to the heuristic correction factor already used in Ref. 22. In our case, the ‘‘correction’’ factor was obtained by a careful counting of the total number m_s of microscopic paths for attachment to small clusters. Also important was a redefinition of the effective island radius R_s as expressed by Eq. (15) in order to satisfy the correct boundary condition in the limit of no detachment.

While our results indicate that the self-consistent rate-equation approach gives significantly improved results for average quantities, the predicted island-size distributions $n_s(\theta)$ remain in poor agreement with simulation results.¹⁶ This is similar to what has been previously observed for the case of irreversible attachment.²⁰ As pointed out in Refs. 20, 22, and 18, this appears to be due to the existence of correlations that modify the size dependence of the capture numbers σ_s although the average capture number σ_{av} remains unchanged. Such correlations have so far not been properly taken into account using a rate-equation formulation, although in Ref. 18 the size dependence of the capture cross section σ_s was measured for a point-island model with irreversible attachment and compared with the corresponding self-consistent rate-equation prediction. The neglect of such correlations may also be the origin of the slight overshoot in the value of χ observed for large Y .

In summary, our self-consistent calculation has led to significantly improved predictions for the average monomer density, island density, and crossover scaling behavior in a model of metal (100) and (111) homoepitaxy. This suggests that a similar approach may be a useful tool in the study of a variety of other systems.

ACKNOWLEDGMENTS

We would like to thank Steve Bales for helpful discussions. This work was supported by National Science Foundation Grant No. DMR-9520842. Part of the KMC simulations used in this work was carried out using the computational facilities of the Cherry L. Emerson Center for Scientific Computation at Emory University.

APPENDIX

The following values for the microscopic detachment rates ω_s and number of attachment paths m_s were used for small clusters: (a) triangular lattice: $\omega_1=0$, $\omega_2=\frac{3}{5}(2r_1D_h)$, and $\omega_s=0$, $s\geq 3$; $m_1=18$. (b) square lattice: $\omega_1=\omega_4=\omega_6=0$, $\omega_2=\omega_3=2r_1D_h$, $\omega_5=\omega_7=r_1D_h$, and $\omega_s=0$, $s\geq 8$; $m_1=12$, $m_2=18$, $m_4=16$, $m_6=18$. We note that these values are appropriate for the case of rapid edge diffusion.

*Present and permanent address: Department of Physics and Astronomy, University of Toledo, Toledo, OH 43606.

¹J. Y. Tsao, *Material Fundamentals of Molecular Beam Epitaxy* (World Scientific, Singapore, 1993).

²Y. W. Mo, J. Kleiner, M. B. Webb, and M. G. Lagally, *Phys. Rev. Lett.* **66**, 1998 (1991).

³H. J. Ernst, F. Fabre, and J. Lapujoulade, *Phys. Rev. B* **46**, 1929 (1992).

⁴R. Q. Hwang, J. Schroder, C. Gunther, and R. J. Behm, *Phys. Rev. Lett.* **67**, 3279 (1991); R. Q. Hwang and R. J. Behm, *J. Vac. Sci. Technol. B* **10**, 256 (1992).

⁵W. Li, G. Vidali, and O. Biham, *Phys. Rev. B* **48**, 8336 (1993).

⁶E. Kopatzki, S. Gunther, W. Nichtl-Pecher, and R. J. Behm, *Surf. Sci.* **284**, 154 (1993).

⁷G. Rosenfeld, R. Servaty, C. Teichert, B. Poelsema, and G. Comsa, *Phys. Rev. Lett.* **71**, 895 (1993).

⁸J. A. Strosio, D. T. Pierce, and R. A. Dragoset, *Phys. Rev. Lett.* **70**, 3615 (1993); J. A. Strosio and D. T. Pierce, *Phys. Rev. B* **49**, 8522 (1994).

⁹J.-K. Zuo and J. F. Wendelken, *Phys. Rev. Lett.* **66**, 2227 (1991); J.-K. Zuo, J. F. Wendelken, H. Durr, and C.-L. Liu, *ibid.* **72**, 3064 (1994).

¹⁰D. D. Chambliss and R. J. Wilson, *J. Vac. Sci. Technol. B* **9**, 928 (1991); D. D. Chambliss and K. E. Johnson, *Phys. Rev. B* **50**, 5012 (1994).

¹¹Q. Jiang and G. C. Wang, *Surf. Sci.* **324**, 357 (1995).

¹²F. Tsui, J. Wellman, C. Uher, and R. Clarke, *Phys. Rev. Lett.* **76**, 3164 (1996).

¹³J. A. Venables, G. D. Spiller, and M. Hanbucken, *Rep. Prog. Phys.* **47**, 399 (1984); J. A. Venables, *Philos. Mag.* **27**, 697 (1973); *Phys. Rev. B* **36**, 4153 (1987).

¹⁴C. Ratsch, A. Zangwill, P. Smilauer, and D. D. Vvedensky, *Phys. Rev. Lett.* **72**, 3194 (1994).

¹⁵J. G. Amar, F. Family, and P. M. Lam, *Phys. Rev. B* **50**, 8781 (1994).

¹⁶J. G. Amar and F. Family, *Phys. Rev. Lett.* **74**, 2066 (1995).

¹⁷M. C. Bartelt and J. W. Evans, *Surf. Sci.* **344**, 1193 (1995).

¹⁸M. C. Bartelt and J. W. Evans, *Phys. Rev. B* **54**, R17 359 (1996).

¹⁹J. G. Amar and F. Family, *Thin Solid Films* **272**, 208 (1996).

²⁰G. S. Bales and D. C. Chrzan, *Phys. Rev. B* **50**, 6057 (1994).

²¹G. S. Bales and A. Zangwill, *Phys. Rev. B* **55**, 1973 (1997).

²²J. G. Amar and F. Family, *Surf. Sci.* **382**, 170 (1997).

²³M. von Smoluchowski, *Z. Phys. Chem., Stoechiom. Verwandtschaftsl.* **17**, 557 (1916); **92**, 129 (1917).

²⁴While the inclusion of a finite barrier to interlayer diffusion may affect the multilayer growth, for the relatively large values of D/F and small submonolayer coverages considered here, there should be little effect on island nucleation.

²⁵The self-consistent rate-equation procedure consists of a numerical integration of Eq. (6) using σ_s and τ_s given by Eqs. (13) along with an iterative self-consistent calculation of ξ and σ_s based on Eqs. (8) and (13a), and a form for R_s at each stage.

²⁶The case $s=1$ is special since from the point of view of a monomer the other monomers have a double hopping rate (Ref. 20). Because of this relative motion, both the left-hand side of Eq. (10) and the capture term in Eq. (10) should be multiplied by 2, while the microscopic detachment rate is $\omega_2=2r_1D_h$. On the other hand, the corresponding RE terms in Eq. (12) both have a factor of 2 due to the loss (formation) of two monomers by the formation (breakup) of a dimer. This explains the presence of the extra factor of 2 in the expression for τ_2^{-1} .

²⁷Z. Zhang, X. Chen, and M. G. Lagally, *Phys. Rev. Lett.* **73**, 1829 (1994).

²⁸We note that while the agreement for the square-lattice case is reasonably good, for the case of rapid edge diffusion the agreement is not quite as good as for the triangular lattice. This may be due to geometrical effects that are more important for the square lattice. In particular, for the square-lattice geometry a correct evaluation of the capture and detachment terms in Eq. (10) for the critical island ($s=3$) involves averaging over possible configurations. To avoid this, we have assumed the most simple form of the cluster (i.e., a linear shape for trimers, neglecting the possibility of an L shape). Taking into account the possibility of an L shape would clearly *decrease* the effective detachment rate and lead to better agreement with simulations.

²⁹C. Ratsch, P. Smilauer, A. Zangwill, and D. D. Vvedensky, *Surf. Sci.* **328**, L599 (1995).

³⁰Here we have used $x_{13}=1.33$ since this gives a better scaling of the KMC data as well as better agreement with the scaling form (2) for the crossover scaling behavior (Ref. 22). As noted in Ref. 22, the use of the value $x_{13}=1.5$ is roughly equivalent to a shift of the RE curves and simulation results in Fig. 5 to the left by a factor of 10.